Differential RCS of Dual-Port Tag Antenna with Synchronous Modulated Backscatter

Nicolas Barbot, Pavel Nikitin

Differential RCS of Dual-Port Tag Antenna with Synchronous Modulated Backscatter

Nicolas Barbot
Univ. Grenoble Alpes, Grenoble INP, LCIS,
F-26000 Valence, France.
nicolas.barbot@lcis.grenoble-inp.fr

Pavel Nikitin
Impinj, Inc
Seattle, WA, USA
nikitin@ieee.org

***Abstract*—This paper introduces a new method allowing one to improve the delta RCS of any passive transponder. By switching simultaneously the loads connected to a dual-port antenna, we show that the associated delta RCS can be higher than the one predicted by the equations of R. Green in 1963. We demonstrate analytically that the delta RCS of the dual-port tag can be improved by 6 dB compared to a single port antenna. This improvement corresponds to an increase of the round-trip read range of 41%. This result can still be improved if the modulation of the structural mode adds constructively with the modulation of the antenna mode. Simulation and measurement of a dual-port tag based on two independent UHF tags validate the model and achieve a large part of the predicted improvement.**

***Index Terms*—Differential Radar Cross-Section (RCS), multi-port antenna, EPC Gen2.**

I. Introduction

Backscattered field of loaded antennas has been analyzed and understood since 1963 by the pioneering work of R. Green [1]. In his thesis, Green successfully decomposes the scattered field of a loaded antenna into a structural mode and an antenna mode. The first contribution is independent of the load connected to the antenna. The latter contribution is proportional to the reflection coefficient between the antenna and the load. However, unlike other decompositions based on short circuit response [2], [3, Eq. (20)], and on open circuit response [4, Eq. (10)], Green's decomposition is based on complex conjugate response [1, Eq. (14)] and can easily be used to predict and bound all possible scattered field values as a function of the load. These concepts have been used and applied in the RFID technology to estimate the scattered field and the efficiency of the transponders. More specifically, the differential RCS (also known as delta RCS) which has been introduced in [5] and extended in [6], has been derived directly from Green's work.

The delta RCS associated to a UHF tag which can switch between two states of complex reflection coefficient Γ_1 and Γ_2 is equal to [1, Eq. (32)], [5, Eq. (6)], [6, Eq. (22)]:

$$\sigma_d = \frac{\lambda^2 G^2}{4\pi} \frac{|\Gamma_1 - \Gamma_2|^2}{4} \tag{1}$$

where λ is the considered wavelength, G is the gain of the antenna and Γ_j is the power wave reflection coefficient between the antenna and the load in the considered state:

$$\Gamma_j = \frac{Z_{cj} - Z_a^*}{Z_{cj} + Z_a} \tag{2}$$

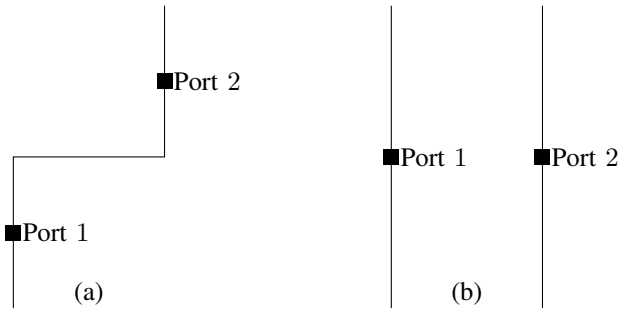

Fig. 1. Example of dual-port antenna: (a) single structure, (b) two separated structures.

Despite its apparent simplicity, note that (1) is valid for any antenna and any load. This quantity is also a bound on the modulated power which can be backscattered towards the reader. From (1), we can see that increasing the delta RCS can only be achieved by increasing the gain, decreasing the frequency, and increasing the distance between Γ_1 and Γ_2. However, each parameter also implies severe constraints on the tag design. For example increasing the gain of the antenna severely limits the position/alignment of the tag. Decreasing the frequency is generally not possible due to local regulations (and also increases the size of the antenna). Finally and more importantly, the distance between Γ_1 and Γ_2, is bounded by 2 for semi-passive tags (and by 1 for passive tags) since $|\Gamma_i|$ is always lower than 1 for any passive loads.

Based on (1) and with the previous assumptions, a classical half-wavelength dipole at 915 MHz has a maximal delta RCS for passive and semi-passive UHF tags of -22.4 dBsm (57.5 cm^2) and -16.4 dBsm (230 cm^2) respectively. Note that all tags presented in the literature are actually bounded by (1). Finally, the design of a tag, (under the considered assumptions) which can achieve a differential RCS higher that the values predicted by (1) remains a open research problem.

The objective of this paper is to design the first passive tag which is not bounded by (1) and which can achieve a differential RCS higher than the one predicted by (1). This design relies on the concept of multi-port tag and multi-port antenna. Multi-port tags are not new in the RFID literature [7], [8]. Usually, these architecture are used to provide diversity in the forward link, which means that if one port experiences

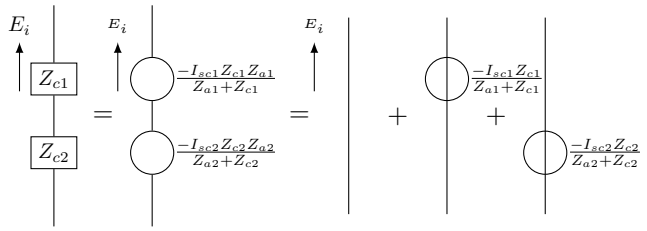

Fig. 2. Decomposition of the field backscattered by a dual-port antenna.

a strong attenuation, the other port can still be used to maintain a given performance. However, in the reverse link, all these works consider that a single port is backscattering at a given time. This condition ensures to avoid any collision between different tags and remains a foundation of the RFID protocol. This work is radically different since the different ports of the system have to backscatter at the same time to benefit from the proposed technique. This can also be seen as a "controlled collision" between different ports which can improve both delta RCS and round-trip read range. This technique is particularly useful for semi-passive tags which are limited by the reader sensitivity.

II. Analytic Model

We consider a dual-port antenna which is characterized by 2 distinct ports. In emission, this antenna can produce an electric field when a voltage (and/or a current) is applied on any of its ports. In reception, this same antenna can generate a voltage (and/or a current) on any of its ports when a wave is impinging the structure. Each port can be loaded by a (passive) complex impedance value. Without any loss of generality, a dual-port antenna can be composed a single structure or multiple structures and ports can be placed anywhere on the structure(s) as presented in Fig. 1.

A. RCS of a Loaded dual-Port Antenna

Field backscattered by a loaded antenna has been known since [1] where Green succeeded to decompose the backscattered field into a structural mode and an antenna mode. This decomposition becomes famous since that all possible amplitude and phase of the backscattered signal can be easily predicted from the load connected to the antenna since Γ is a bounded quantity. Note that this derivation also assumes a single port antenna. Consequently, delta RCS of a single-port antenna can, by definition, not be higher than (1).

On the other side, if we consider the delta RCS of an antenna with more than one port, then this quantity is, by design, not bounded by (1) if both loads can be modified at the same time. The following of this section generalizes the procedure discovered by Green in the case of a dual-port antenna.

By using the compensation theorem and then the superposition theorem, the field backscattered by a dual-port antenna can be decomposed into the field backscattered by the antenna with a short circuit on both ports plus the field generated by each port loaded by a voltage generator while the other port is short circuited (see Fig. 2):

$$E_s(Z_{c1},Z_{c2}) = E_s(0,0) - \frac{Z_{c1}I_{sc1}}{Z_{c1}+Z_{a1}}E_{r1} - \frac{Z_{c2}I_{sc2}}{Z_{c2}+Z_{a2}}E_{r2} \tag{3}$$

By using (3) with (Z_{a1}^*, Z_{a2}^*), we can express $E_s(0,0)$ by:

$$E_s(0,0) = E_s(Z_{a1}^*,Z_{a2}^*) + \frac{Z_{a1}^*}{2R_{a1}}I_{sc1}E_{r1} + \frac{Z_{a2}^*}{2R_{a2}}I_{sc2}E_{r2} \tag{4}$$

Also, I_{sc1} and I_{sc2} can be expressed as a function of the conjugate currents:

$$I_{sc1} = I_1(Z_{a1}^*)\frac{2R_{a1}}{Z_{a1}} \quad \text{and} \quad I_{sc2} = I_2(Z_{a2}^*)\frac{2R_{a2}}{Z_{a2}} \tag{5}$$

Thus, $E(0,0)$ can be expressed only with the conjugate currents:

$$E_s(0,0) = E_s(Z_{a1}^*,Z_{a2}^*) + \frac{Z_{a1}^*}{Z_{a1}}I_1(Z_{a1}^*)E_{r1} + \frac{Z_{a2}^*}{Z_{a2}}I_2(Z_{a2}^*)E_{r2} \tag{6}$$

Finally, (6) can be reinjected into (4):

$$\begin{aligned} E_s(Z_{c1},Z_{c2}) &= E_s(Z_{a1}^*,Z_{a2}^*) && (7)\\ &\quad + \frac{1}{Z_{a1}}\left[Z_{a1}^* + \frac{2R_{a1}Z_{c1}}{Z_{a1}+Z_{c1}}I_1(Z_{a1}^*)E_{r1}\right] && (8)\\ &\quad + \frac{1}{Z_{a2}}\left[Z_{a2}^* + \frac{2R_{a2}Z_{c2}}{Z_{a2}+Z_{c2}}I_2(Z_{a2}^*)E_{r2}\right] && (9)\\ &= E_s(Z_{a1}^*,Z_{a2}^*) && (10)\\ &\quad - \Gamma_1 I_1(Z_{a1}^*)E_{r1} - \Gamma_2 I_2(Z_{a2}^*)E_{r2} && (11) \end{aligned}$$

where Γ_i is the reflection coefficient at the considered port i:

$$\Gamma_1 = \frac{Z_{c1}-Z_{a1}^*}{Z_{c1}+Z_{a1}} \quad \text{and} \quad \Gamma_2 = \frac{Z_{c2}-Z_{a2}^*}{Z_{c2}+Z_{a2}} \tag{12}$$

The RCS of the dual-port antenna can finally be extracted:

$$\sigma = 4\pi r^2 \frac{|E_s(Z_{a1}^*,Z_{a2}^*) - \Gamma_1 I(Z_{a1}^*)E_{r1} - \Gamma_2 I(Z_{a2}^*)E_{r2}|^2}{|E_i|^2} \tag{13}$$

This RCS can also be expressed as a function of antenna "gains".

$$\sigma = \frac{\lambda^2}{4\pi}\cdot|A - G_{m1}e^{j\phi_1}\Gamma_1 - G_{m2}e^{j\phi_2}\Gamma_2|^2 \tag{14}$$

with:

$$A = \frac{4\pi}{\lambda}E_s(Z_{a1}^*,Z_{a2}^*) \tag{15}$$

$$G_{mi} = \frac{4\pi}{\lambda}|I_i(Z_{ai}^*)E_{ri}| \tag{16}$$

$$\phi_i = \arg(I_i(Z_{ai}^*)E_{ri}) \tag{17}$$

Note that G_{mi} are not equal to the gains of the antenna at port i but are different quantities. Fig. 3 presents the different quantities graphically. Note that the structural mode is not bounded. The antenna mode of the first port is bounded by a circle of radius G_{m1}. The antenna mode of the second port is bounded by a circle of radius G_{m2}. The total antenna mode corresponding to the summation of each port is bounded by a radius of $G_{m1}+G_{m2}$. Finally the square root of the RCS of the dual-port antenna is proportional to the length between $-A$ and the total antenna mode.

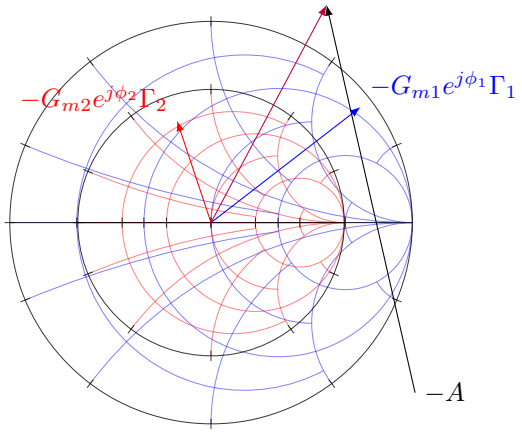

Fig. 3. Graphical representation of the scattering of a dual-port antenna. Square root of the RCS of the dual-port antenna is proportional to the length of the black plain line.

B. Delta RCS of a dual-Port Tag

Let's now imagine that each port of this dual-port antenna can be switched between two values:

$$\begin{cases} Z_{c1} \rightarrow (Z_{c11}, Z_{c12}) \\ Z_{c2} \rightarrow (Z_{c21}, Z_{c22}) \end{cases} \tag{18}$$

Note that the impedance change have to appears at the same time on both ports. This condition is particularly important because if a single port is switched at a given time, the delta RCS associated to each variation is directly given by (1) and can not be improved.

By applying (11) for both states and then doing the difference, the total field variation can be obtained by:

$$\begin{aligned} \Delta E_s = {} & E_s(Z_{a11}^*, Z_{a21}^*) - E_s(Z_{a12}^*, Z_{a22}^*) \\ & - \Gamma_{11} I_1(Z_{a11}^*) E_{r11} - \Gamma_{21} I_2(Z_{a21}^*) E_{r21} \\ & + \Gamma_{12} I_1(Z_{a12}^*) E_{r12} + \Gamma_{22} I_2(Z_{a22}^*) E_{r22} \end{aligned} \tag{19}$$

The quantity expressed by (19) can be normalized to obtain the delta RCS of the dual-port antenna:

$$\begin{aligned} \sigma_d = {} & \pi r |E_s(Z_{a11}^*, Z_{a21}^*) - E_s(Z_{a12}^*, Z_{a22}^*) \\ & + \Gamma_{12} I_1(Z_{a12}^*) E_{r12} + \Gamma_{22} I_2(Z_{a22}^*) E_{r22} \\ & - \Gamma_{11} I_1(Z_{a11}^*) E_{r11} - \Gamma_{21} I_2(Z_{a21}^*) E_{r21}|^2 / |E_i|^2 \end{aligned} \tag{20}$$

Equation (20) can also be expressed as a function of G_m:

$$\begin{aligned} \sigma_d = \frac{\lambda^2}{16\pi} | & A_1 - A_2 \\ & + G_{m12} e^{j\phi_{12}} \Gamma_{12} + G_{m22} e^{j\phi_{22}} \Gamma_{22} \\ & - G_{m11} e^{j\phi_{11}} \Gamma_{11} - G_{m21} e^{j\phi_{21}} \Gamma_{21}|^2 \end{aligned} \tag{21}$$

with:

$$A_j = \frac{4\pi}{\lambda} E_s(Z_{a1j}^*, Z_{a2j}^*) \tag{22}$$

$$G_{mij} = \frac{4\pi}{\lambda} |I_{ij}(Z_{aij}^*) E_{rij}| \tag{23}$$

$$\phi_{ij} = \arg(I_1(Z_{aij}^*) E_{rij}) \tag{24}$$

Equation (21) is the general form of the delta RCS of a dual-port antenna. The term $A_1 - A_2$ is a modulation due to the variation of the structural mode. This term was not present for single-port antenna [see (1)]. Each following terms are proportional to Γ_{ij} and corresponds to the modulation of the antenna mode produced by the two ports. This delta RCS has to be compared with the one of the single-port antenna given by (1). The direct analysis of (21) states that if we can find a dual-port antenna having good "gains" on both ports ($G_{mij} \approx G$), then delta RCS of a dual-port antenna can be improved by a factor of 4 (*i.e.* +6 dB) compared to a single-port antenna. This quantity can still be improved if the modulation due to the structural mode adds constructively. In term of read range, assuming a free space environment, an increase of the delta RCS of 6 dB represents an improvement of 41% of the round trip read range [9] compared to a single-port tag.

III. Simulation

In the following, we consider 2 parallel and identical dipoles in free space separated by a distance of 20 cm. Each dipole can be loaded at its center by a complex load. Dipole length has been set to 15 cm which is approximately equal to $\lambda/2$ at 915 MHz. Simulations have been realized with NEC2, which is based on the Method of Moment. Each dipole has been modeled by 11 segments using the thin wire approximation. The structure is impinged by a plane wave at 915 MHz face to the dipoles, and backscattered field E_s is collected using a farfield probe located at 1 m. Two scenarios have been considered which are the "single-port tag" and the "dual-port tag". In the single-port tag, a single-port is switched (from $Z_{c11} = 10 + 100i\ \Omega$ to $Z_{c11} = 10 - 100i\ \Omega$) while the other port remains constant ($Z_{c21} = Z_{c22} = 10 + 100i\ \Omega$), this case corresponds to the classical case and is presented as a reference. In the dual-port case, both ports are switched simultaneously (from $Z_{c11} = Z_{c21} = 10 + 100i\ \Omega$ to $Z_{c12} = Z_{c22} = 10 - 100i\ \Omega$). See the two first lines of each subtable of Table I.

Delta RCS have been estimated directly from the E_s values by running two independent simulations corresponding to two different time slots. Results are presented in the Simulated σ_d line in both subtables of Table I. Delta RCS have been also determined from the analytic model. Determination is based on (1) and (21) for the single-port tag and the dual-port tag respectively. Independent simulations have been performed to determine the values of each parameter of (21) [and (1)] (*i.e.*, Z_{ai}, Γ_i, E_{ri}, $I_1(Z_{aij}^*)$, A, G_{mi} and ϕ_i). Moreover, since the simulation considers two identical chips, then $Z_{c11} = Z_{c21}$ and $Z_{c12} = Z_{c22}$. Also, since antenna is identical for both tags, then $Z_{a1} = Z_{a2}$. Consequently, $\Gamma_{11} = \Gamma_{21}$ and $\Gamma_{12} = \Gamma_{22}$. In addition, due to the symmetry in the structure, $G_{m11} = G_{m21}$ and $G_{m12} = G_{m22}$. Thus, delta RCS expression given by (21), for the proposed structure, can be further simplified as:

$$\sigma_d = \frac{\lambda^2}{4\pi} \frac{|A_1 - A_2 - 2G_{mi1} e^{j\phi_{i1}} \Gamma_{i1} + 2G_{mi2} e^{j\phi_{i2}} \Gamma_{i2}|^2}{4} \tag{25}$$

TABLE I
SIMULATION OF A SINGLE-PORT TAG AND A DUAL-PORT TAG.

SINGLE-PORT TAG

	Time slot 1	Time slot 2
Z_{c1} (Ω)	$10+100i$	$10-100i$
Z_{c2} (Ω)	$10+100i$	$10+100i$
E_s (V/m)	$-0.115696-0.040380i$	$-0.009681-0.071512i$
Simulated σ_d (dBsm)	-14.162	
Z_a (Ω)	$60.210-25.010i$	$60.210-25.010i$
Γ	$0.19883+0.85571i$	$0.53693-0.76938i$
E_r (V/m)	$-28.256-62.154i$	$-11.332-56.615i$
$I(Z_a^*)$ (mA)	$0.98039+0.22602i$	$0.98039+0.22602i$
G	2.5823	2.5823
Analytic σ_d (dBsm)	-14.187	

DUAL-PORT TAG

	Time slot 1	Time slot 2
Z_{c1} (Ω)	$10+100i$	$10-100i$
Z_{c2} (Ω)	$10+100i$	$10-100i$
E_s (V/m)	$-0.115696-0.040380i$	$0.062303-0.055823i$
Simulated σ_d (dBsm)	-9.9874	
Z_{a1} (Ω)	$60.210-25.010i$	$67.330-28.481i$
Z_{a2} (Ω)	$60.210-25.010i$	$67.330-28.481i$
Γ_1	$0.19883+0.85571i$	$0.53693-0.76938i$
Γ_2	$0.19883+0.85571i$	$0.53693-0.76938i$
E_{r1} (V/m)	$-28.256-62.154i$	$-11.332-56.615i$
E_{r2} (V/m)	$-28.256-62.154i$	$-11.332-56.615i$
$I_1(Z_{aij}^*)$ (mA)	$0.93545+0.05696$	$0.87925+0.02067i$
$I_2(Z_{aij}^*)$ (mA)	$0.93545+0.05696$	$0.87925+0.02067i$
A	$-0.8634-3.9601i$	$-0.9236-3.6796i$
G_{m1}	2.4524	1.9463
G_{m2}	2.4524	1.9463
ϕ_1 (rad)	-1.9367	-1.7448
ϕ_2 (rad)	-1.9367	-1.7448
Analytic σ_d (dBsm)	-9.9881	

Note that this expression is valid only for the considered structure (2 parallel identical tags face to the reader). For a general dual-port tag, (21) has to be used. Results are presented in the Analytic σ_d line in both subtable of Table I. We can easily verify that the simulation and the analytic expression are in very close agreement (slight difference appears at the second digit after the comma) for both single-port and dual-port tag. Finally, the delta RCS value of the dual-port tag, in simulation and predicted by (21), is 4.2 dB higher than the delta RCS of a single-port tag. This results proves that the delta RCS of a dual-port tag is not bounded by (1) and can be higher that classical values considered in UHF RFID.

IV. PROOF OF CONCEPT

A. Dual-Port Tag

Dual-port tags can be realized using at least two backscatter modulators. Designs can be obtained from [10] for example by adding a second backscatter modulator. In this paper, we do not propose a fully compliant dual-port tag compatible with the Gen2 protocol but a proof of concept.

A dual-port-tag can be simply designed using 2 independent UHF tags. By ensuring that both tags respond at the (exact) same time, a dual-port tag can be emulated from the two independent tags. Note that, as we will see in Section IV-B, this condition requires some precautions with the Gen2 protocol. Thus, two identical tags based on the Impinj E62 Reference Design (Monza R6 chip) have been selected. Moreover, the auto tuning functionality has been disabled on both chips. A picture of the proposed dual-port tag is presented in the inset of Fig. 4. Note that the proposed design can not be used to extract a (single) EPC due to the random nature of the Gen2 protocol. However delta RCS of this dual-port tag can be estimated and compared to the case where a single tag is read.

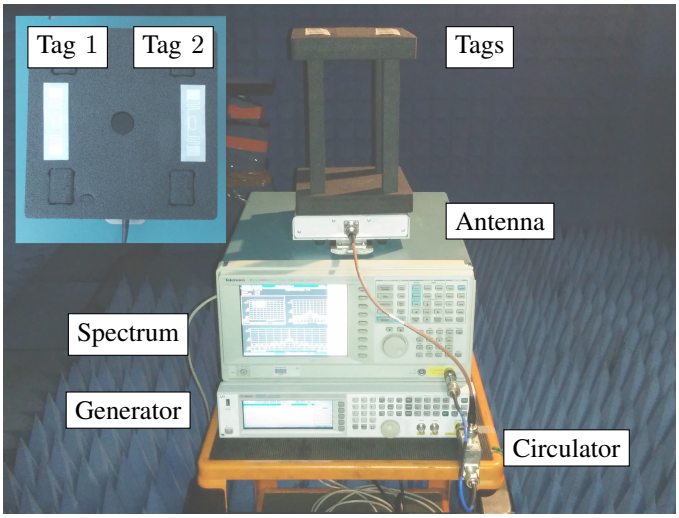

Fig. 4. Photograph of the proposed bench based on a monostatic configuration in anechoic chamber. Inset: Proposed dual-port tag composed of two identical tags.

B. Measurement Bench

The measurement bench is based on a vector signal generator and a real time spectrum analyzer [11]. In transmission, the generator transmits a signal to the antenna through a circulator. In reception, the signal received from the antenna is directed to the spectrum analyzer. Both instruments share the same 10 MHz reference clock signal and are controlled by a single script executed on a remote PC. Moreover a trigger from the generator to the spectrum allows one to synchronize the acquisition. A picture of the developed bench is presented in Fig. 4.

In order to characterize the performance of the dual-port tag and compare it to a classical single-port tag, specific commands have to be issued to interrogate the tags. Three different cases have been explored. The first one corresponds to the interrogation of the first tag (Tag 1). The second one corresponds to the interrogation of the second tag (Tag 2). The last case corresponds to the interrogation of both tag at

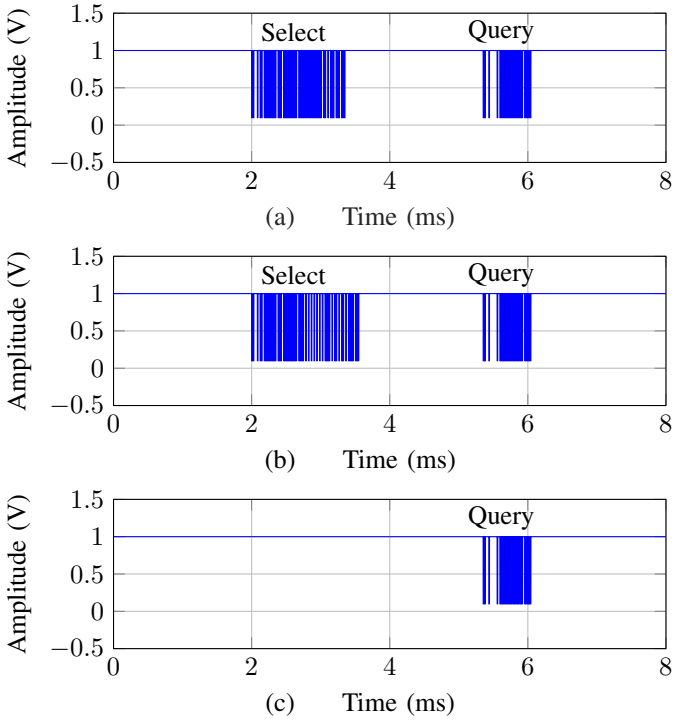

Fig. 5. Commands generated by the proposed bench: (a) Tag 1, (b) Tag 2, (c) both tags.

the same time. In order to interrogate a single tag, a select command [12, Section 6.3.2.12.1.1] is first issued to filter a single tag according to (a part of) its EPC, then a query command [12, Section 6.3.2.12.2.1] with a single slot is issued in the corresponding session to read the chosen tag. The reading of both tags at the same time is more challenging since the RFID protocol is designed to avoid tag collision. Thus, to produce a collision, a query is generated using a single slot [12, Figure 6.18]. If the two tags are in the ready state [12, Figure 6.21], they will both respond in the same slot. Fig. 5 summarizes the different inventory rounds realized to read the tags. Note that after each inventory round, selected tag(s) will backscatter their RN16 which is captured by the spectrum analyzer in the time domain. All data are processed on the remote PC. This technique allows one to characterize each configuration without touching or moving the tags.

Response backscattered by the tag(s) are presented in Fig. 6. Note that the data associated to each response is a random number on 16 bits which is chosen by the pseudo random number generator present inside each chip. Note that the amplitude and phase of the signal is affected during the load modulation. We can see that the amplitude variation of Tag 1 and Tag 2 are almost identical. However when both tags are modulating, the amplitude variation is increased compared to the single tag response. Moreover this latter response can be decomposed into two parts. The first one corresponds to the preamble `1010v1` [12, Figure 6-11]. This part can be easily decoded since both tags are backscattering at the

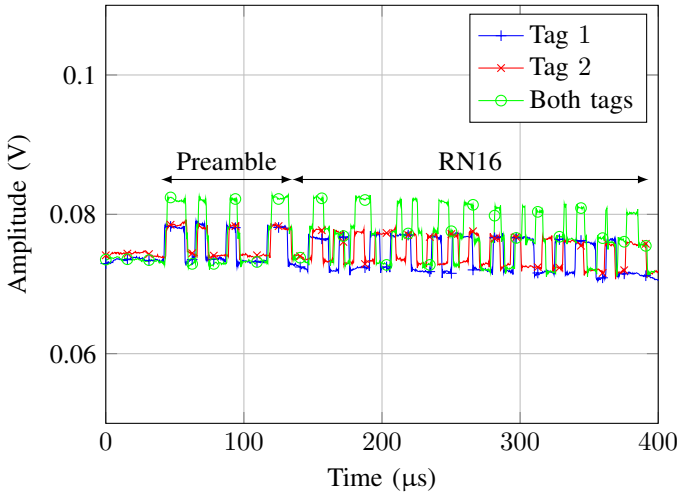

Fig. 6. Amplitude of the backscattered RN16 as a function of time at 915 MHz: (a) Tag 1, (b) Tag 2, (c) both tags.

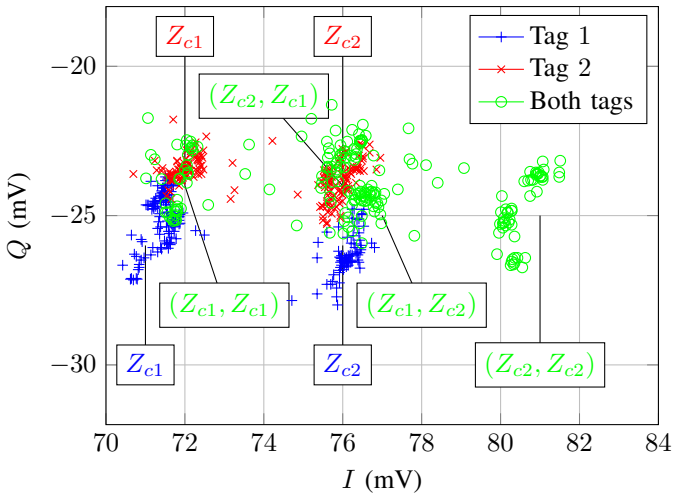

Fig. 7. Constellation of the backscattered RN16 in the IQ plan between 300 and 400 us at 915 MHz: (a) Tag 1, (b) Tag 2, (c) both tags.

same time the same data. The second part corresponds to the RN16. Note that this part is different for each tag (different data) resulting in four different amplitude levels. Also, one can remark that during the preamble, both tags are switching their loads at the same time whereas this condition is not always respected for the RN16. Finally, a dual-port tag can be emulated by considering these two independent tag as a single dual-port tag during the preamble (or during the RN16 but by considering transition from (Z_{c1}, Z_{c1}) and (Z_{c2}, Z_{c2}) only). The associated delta RCS of this dual-port tag can thus be extracted from the preamble of the collided response.

In order to extract the differential RCS, note that both amplitude and phase variation of the backscattered signal should be considered. Fig. 7 presents the response in each considered case in the IQ diagram during the RN16. This figure presents the same results as Fig. 6 but allows one to easily derive the delta RCS. Single tags are composed of a constellation

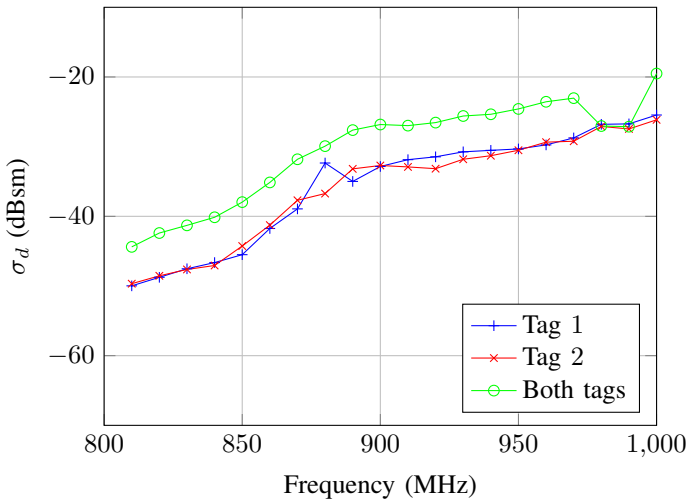

Fig. 8. Delta RCS as a function of the frequency: (a) Tag 1, (b) Tag 2, (c) both tags.

of two points. On the other side, the constellation associated to the (non synchronous) dual-port tag is composed of four points corresponding to the four combinations of the tags (*i.e.*, (Z_{c1}, Z_{c1}), (Z_{c1}, Z_{c2}), (Z_{c2}, Z_{c1}) and (Z_{c2}, Z_{c2}). Note that due to the symmetry of the structure, combinations (Z_{c1}, Z_{c2}) and (Z_{c2}, Z_{c1}) produce almost the same amplitude and phase for the backscattered signal. Moreover the distance between (Z_{c1}, Z_{c1}) and (Z_{c2}, Z_{c2}) is more important compared to the distance between the two points of any single tag. In Fig. 7, this distance is improved from 4 mV to 8 mV for a single-port tag and a dual-port tag respectively. In power, this represents an improvement of $+6$ dB which is in agreement with the prediction of the analytical model. Thus modulation efficiency of the dual-port tag is improved compared to a single-port tag (using the same chip).

Finally, the last study is presented in Fig. 8 and plots the evolution of the delta RCS as a function of the frequency for the two single-port tags and for the dual-port tag. Measurement procedure is similar to [11] with a static calibration. Note that this delta RCS has been evaluated at the activation power at each frequency. Delta RCS values between 800 MHz and 1 GHz are similar for Tag 1 and Tag 2. On the other side, delta RCS of the dual-port tag is 6 dB higher than the one of a single-port tag. This improvement have been observed over the whole band.

V. Discussion

The proposed design is able to verify the analytic model and to prove that the delta RCS of a dual-port tag can be higher than the one associated to a single-port tag (*i.e.*, all classical UHF tags) if multiple ports are switched simultaneously. However the proposed proof of concept based on two independent tags suffers from important limitations. Since the design is based on two independent chips, each chip operates independently from each other, thus even if the same EPC is written inside the chip memories, the proposed tag can not be read easily by a reader due to the random characteristics of the RFID protocol. Thus, even if the reader use a single slot inventory, this dual-port tag can not easily be read since the probability that the two RN16 are equal is quite low. By considering a single slot inventory round of 10 ms, this dual-port tag could theoretically be read once every 11 min on average.

VI. Conclusion

This paper shows that the delta RCS of a transponder can be improved if we modulate simultaneously multiple ports of its antenna. This contribution can allow tag designers to increase the delta RCS of a transponder by a factor 4 (*i.e.*, $+6$ dB) which corresponds to a round-trip read range improvement of 41%. The concept has been verified in simulation and measurement. A first proof of concept has been realized using 2 independent tags to validate the delta RCS improvement However, complete reading of a tag has not been done yet (only RN16 have been investigated). Additional work to read the full EPC of a dual-port tag is still needed to realize the full potential of this technique.

A natural perspective to this work will be to combine multi-port harvester and multi-port backscatter modulator into a single chip. This architecture could represents an interesting candidate for the next generation of RFID chips.

Acknowledgment

This work has been supported by the Auvergne Rhone Alpes Region through the PAI Horizon-TA.

References

[1] R. B. Green, "The general theory of antenna scattering," Ph.D. dissertation, The Ohio State University, Electrical Engineering., OH, USA, 1963.

[2] R. King and C. Harrison, "The receiving antenna," *Proceedings of the IRE*, vol. 32, no. 1, pp. 18–34, Jan. 1944.

[3] R. Hansen, "Relationships between antennas as scatterers and as radiators," *Proceedings of the IEEE*, vol. 77, no. 5, pp. 659–662, May 1989.

[4] R. Collin, "Limitations of the Thevenin and Norton equivalent circuits for a receiving antenna," *IEEE Antennas and Propagation Magazine*, vol. 45, no. 2, pp. 119–124, Apr. 2003.

[5] P. Nikitin, K. V. S. Rao, and R. D. Martinez, "Differential RCS of RFID tag," *Electron. Lett.*, vol. 43, no. 8, pp. 431–432, Apr. 2007.

[6] N. Barbot, O. Rance, and E. Perret, "Differential RCS of modulated tag," *IEEE Trans. Antennas Propag.*, vol. 69, no. 9, pp. 6128–6133, Sep. 2021.

[7] G. Marrocco, "RFID grids: Part I – electromagnetic theory," *IEEE Transactions on Antennas and Propagation*, vol. 59, no. 3, pp. 1019–1026, Mar. 2011.

[8] S. Caizzone and G. Marrocco, "RFID grids: Part II – experimentations," *IEEE Transactions on Antennas and Propagation*, vol. 59, no. 8, pp. 2896–2904, Oct. 2011.

[9] N. Barbot, I. Prodan, and P. Nikitin, "A practical guide to optimal impedance matching for UHF RFID chip," *IEEE Journal of Radio Frequency Identification*, pp. 1–1, 2024.

[10] N. Barbot and P. Nikitin, "Simple open-source UHF RFID tag platform," in *2023 IEEE International Conference on RFID (RFID)*, Seattle, WA, Jun. 2023, pp. 78–83.

[11] N. Barbot and V. C. V, "Open testing and measurement bench for UHF RFID," in *2023 IEEE 13th International Conference on RFID Technology and Applications (RFID-TA)*, Aveiro, Portugal, Sep. 2023, pp. 158–161.

[12] EPC Radio-Frequency Identity Generation-2 UHF RFID Standard, Specification for RFID Air Interface Protocol for Communications at 860 MHz – 930 MHz, Release 3.0, Ratified, Jan 2024.